2021 18th International Conference on Electrical Engineering, Computing Science and Automatic Control (CCE). Mexico City, Mexico. November 10-12, 2021

Numerical Study of the Recombination Profiles in CIGSe Thin Film Solar Cells Through Silvaco Atlas Simulator after using Experimental Parameters

D. Valencia, M. Zuñiga, C. Meza-Avendaño, I. Zuñiga, H. Vilchis
Institute for Research and Innovation in Renewable Energies, UNICACH, Tuxtla Gutierrez, Chiapas, Mexico
ldorian.valor@gmail.com

J. Conde
CONACYT - *Institute for Research and Innovation in Renewable Energies, UNICACH, Tuxtla Gutierrez,* Chiapas, Mexico
jorge.conde@unicach.mx

A. Ashok, S. Velumani
Dep. of Electrical Engineering, CINVESTAV-IPN, Zacatenco, Mexico City, Mexico
ashokad@cinvestav.mx
velu@cinvestav.mx

***Abstract*— Solar energy is one of the very promising renewable energy sources, which can provide tremendous energy for a long period. Besides, it is non-pollutant and available freely. Solar energy can replace the potential to replace the non-renewable energy source for energy production. Among the various generation of the photovoltaic (PV) technology, the $CuInGaSe_2$ (CIGSe) is a thin film solar cell (TFSC) has attracted for transferring solar energy into the electrical energy. The recent focus on the CIGSe based TFSC is due to its material properties that can reduce the cost and improve the device performance. In this study, the high photovoltaic cell efficiency (PCE) of CIGSe TFSC is first optimized through the Silvaco Atlas simulator. A maximum PCE of 21.92 % is observed from the simulation. Then the device performance and recombination profiles are studied after replacing the experimental parameters of the CIGSe absorber layer. Afterward, a similar study is carried out after substituting the experimental parameters of CIGSe absorber layer and CdS buffer layer. The PCE of 15.01% is observed after replacing the experimental parameters of CIGSe and CdS with the optimized condition, which is lower than the optimized conditions showing the presence of recombination centers in the device. Hence, analyzing these simulated results can guide information about the best material parameters which contain fewer defects and good quality.**

Keywords*— $CuInGaSe_2$ (CIGSe) TFSC, hybrid deposition method, numerical simulation, Silvaco Atlas,

I. INTRODUCTION

The use of energy can enhance the nation's development. For worldwide energy production, Non-renewable energy sources have been consuming as major energy sources. The search for alternative energy sources for non-renewable energy has been rising due to the limited quantity available on the earth and its impact on the environmental system. Renewable energy sources are an alternative option for replacing non-renewable energy sources. Solar energy is one of the most favorable renewable energy sources. Solar cells in Photovoltaic (PV) technologies can directly convert solar energy into useful electrical energy. Various generations are of PV technologies are found [1]. Among them, silicon-based solar cells have been dominating the PV market for energy conversion. But the fabrication cost of the silicon-based device is high. So, new materials and technology are needed to reduce the device cost. The CIGSe based thin-film solar cells can be promising in the PV market due to their long-term thermal stability, high absorption coefficient, high radiation hardness on electrons and holes, high yield per weight, and high record efficiency (23.35%) [2], [3].

There are various deposition techniques available for CISe/CIGSe thin films. Those deposition techniques are normally divided into vacuum and non-vacuum-based methods. Although vacuum-based methods provide high PCE, the fabrication cost of the material is high in vacuum methods. Low-cost non-vacuum methods are also containing the disadvantages of the low PCE of the device. Therefore, a novel technique is required to resolve both disadvantages observed in vacuum and non-vacuum methods. For this, this study applies a hybrid deposition method that combines both vacuum co-evaporation and non-vacuum spray pyrolysis methods. The purpose of using the hybrid method is to reduce the cost by utilizing low-cost materials and reducing the waste of pure materials. Optimizing the best deposition condition is time-consuming and costly. A new approach like a theoretical model is necessary to optimize the best material properties used in solar cells.

For interpreting the physical phenomena and behaviors of semiconductor devices, numerical simulation has been recently attracted. The numerical simulation usually is cheaper and quicker for analyzing the device performance than experimental work. All the semiconducting parameters are well-controlled in the simulation that can examine the properties of semiconducting materials that are difficult or impossible to study experimentally. Various numerical simulations are available to investigate the device performance, tunneling, recombination profiles, and other characteristics [4]–[6]. All these simulations are used for different applications. Generally, these simulators are designed to explain the basic semiconductor equations (i.e., Poisson's equation and Continuity equations) for charge carriers and produce non-linear equations that can be used to model solar cells. Among various simulations, Silvaco Atlas is one of the best simulators that can concisely study the device's performance. It can offer 2D or 3D semiconductors' designs and calculates the optical and electrical characteristics. Besides, it can have a remarkable promise for designing and optimizing solar cells. The effect of material properties on the device performance can be analyzed and provide an idea for practical work.

978-1-6654-0029-9/21/$31.00 ©2021 IEEE

In this study, the Silvaco Atlas simulator designs and simulates the CdS/CIGSe heterojunction TFSC. The CIGSe TFSC is optimized for high PCE. Experimental parameters of CIGSe and CdS are replaced with the optimized condition and also checked the recombination profiles. This model can provide an idea for optimizing the deposition condition and improving the device performance in the future.

II. EXPERIMENTAL AND SIMULATIVE DETAILS

A. Experimental details

The CIGSe thin films were deposited by the novel hybrid deposition method. This proposed hybrid deposition method (see Fig. 1a) consists of 3 stages, combining pneumatic spray pyrolysis technique for the first stage and co-evaporation method for the 2nd and 3rd stages. The $(In, Ga)_2Se_3$ thin films were deposited in the first stage of the hybrid deposition method. The substrate temperatures used for $(In, Ga)_2Se_3$ thin films deposition were in the range of 320-340 ˚C with the step of 10 ˚C. A brief description of the optimized deposition condition for $(In, Ga)_2Se_3$ thin films by pneumatic spray pyrolysis can be found in [7][8].

In the second stage, copper and selenium were co-evaporated over the $(In, Ga)_2Se_3$ precursor layer. The grain size of thin films will enhance after the 2nd stage through the recrystallization phenomenon. The bigger grains in the films help reduce the number of grain boundaries and enhance the performance by decreasing recombination centers for generated charge carriers. The 3rd stage of the hybrid deposition method involves the co-evaporation of indium, gallium, and selenium. After the 3rd stage, the composition of the thin film will reach a slightly poor copper composition which is required for getting a p-type absorber layer. The deposition parameters used in the co-evaporation method such as base chamber pressure, substrate temperature, copper source temperature, indium source temperature, gallium source temperature, selenium source temperature, and distance between the source element and the substrate holder are 5×10^{-6} Torr, 550 ˚C, 1300 ˚C, 950 ˚C, 850 ˚C, 250 ˚C, and 30 cm, respectively.

Subsequently, the complete CIGSe thin films were selenized in an MTI vacuum oven for increasing grain size and getting homogenous distribution of elements throughout the films. The two-step selenization processes were employed, containing an initial lower temperature selenization (450-500 ˚C) for 15 minutes followed by the higher temperature selenization (500-550 ˚C) for 30 minutes were employed. The selenization process was done in an argon gas environment to prevent extra chemical reactions while selenizing CIGSe thin films. The thickness, structural, morphological, compositional, topographical, and electrical properties were estimated by Bruker profilometry DektarXT, Bruker XRD-D2 phaser, Tescan Vega-3 SEM fitted with Bruker EDX, NTMDT Ntegra spectra, and Hall-van der Pauw method, respectively.

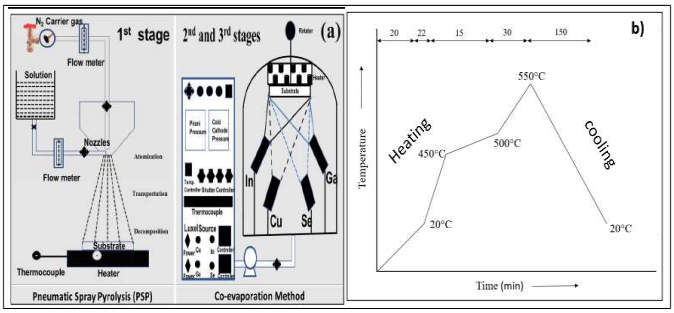

Fig. 1. Schematic of (a) hybrid deposition method (b) selenization process for CIGSe absorber layer

B. Silvaco Atlas simulation details

The Silvaco Atlas simulation is 2D or 3D, mainly based on the Poisson equation and the continuity equations for charge carriers. The CIGSe thin film solar cells were simulated using Silvaco Atlas software. Fig. 2 depicts the 2D mesh and CIGSe TFSC used in the Silvaco Atlas simulation. The 2D mesh structure displays different regions assigned to the materials, the electrodes, and the light spectrum specification. The horizontal and vertical lines with a user-defined spacing between them are observed in the 2D mesh. The CIGSe TFSC structure consists of molybdenum as a back contact, CIGSe as an absorber layer, CdS as a buffer layer, i-ZnO as a window layer, ZnO: Al as a transparent conducting oxide, and finally, Ni/Al/Ni as a front contact. The effect of different layer parameters such as thickness, bandgap, carrier concentration, mobility, resistivity, etc., on the device performance and recombination profiles, was simulated and analyzed. The simulated study in Silvaco Atlas was performed under AM 1.5G solar spectrum (corresponds light energy density of 1000 W/m^2) at ambient temperature. The material properties utilized in the simulation study to optimize high CIGSe TFSC performance are presented in Table I [9]–[11]. The simulated parameters for each layer of CIGSe TFSC are thickness (t), bandgap (E_g), dielectric constant (ε_r), mobilities (μ_e and μ_h), carrier concentrations (N_D and N_A), the effective density of states in conduction and valence band (N_C and N_V), and recombination lifetimes (τ_e and τ_h). The extracted tail and deep defect parameters for exponential tail distributions and Gaussian distributions were summarized in Table II [12]–[14]. These parameters were optimized for achieving as high device performance as possible. Then, the experimental parameters of CIGSe and CdS thin films were replaced with the optimized condition. The solar cell parameters and recombination profiles after replacing experimental parameters were studied.

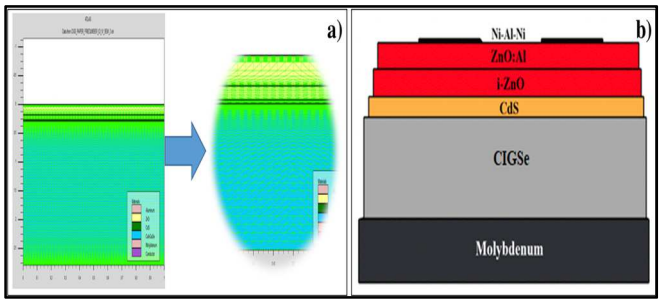

Fig. 2. Schematic of the a) 2D mesh, b) CIGSe TFSC structure used in Silvaco Atlas simulator

Table I. MATERIAL PARAMETERS USED IN THE NUMERICAL SIMULATION FOR CIGSe TFSC

Parameters	CIGSe	CdS	i-ZnO	ZnO: Al
t (nm)	1300-3000	23	85	180
E_g (eV)	1.035-1.675	2.45	3.25	3.25
χ_e (eV)	3.86-4.55	4.28	4.55	4.5
ε_r	13.6	10	9	9
N_{CB} (cm^{-3})	2.2E18	2.2E18	3.5E18	3.5E18
N_{VB} (cm^{-3})	1.8E19	1.46E19	8.8E18	8.8E18
μ_e (cm^2/Vs)	100	25	25	100
μ_h (cm^2/Vs)	25	5	5	31
N_D (cm^{-3})	1E16	1E18	1E17	1E20
N_A (cm^{-3})	1E14-8E16	0	1E17	0
τ_e (s)	1E-7	1E-9	1E-9	1E-9
τ_h (s)	1E-8	1E-10	1E-10	1E-10

Table II TAIL AND DEEP DEFECT PARAMETERS

	CIGSe	CdS	i-ZnO	ZnO:Al
Donors				
N_{TD} (cm^{-3} eV^{-1})	7E18	1.87E20	5E18	5E17
N_{GD} (cm^{-3} eV^{-1})	8E13	1E16	1E15	1E15
E_{GD} (eV)	0.65	1.225	1.625	1.625
W_{TD} (eV)	0.01	0.01	0.01	0.01
W_{GD} (eV)	0.1	0.1	0.1	0.1
SIGTDE (cm^2)	5E-13	1E-10	5E-13	5E-13
SIGTDH (cm^2)	1E-15	1E-10	1E-15	1E-15
SIGGDE (cm^2)	5E-13	1E-10	5E-13	5E-13
SIGGDH (cm^2)	1E-15	1E-10	1E-15	1E-15
Acceptors				
N_{TA} (cm^{-3} eV^{-1})	2E18	4.38E19	6.8E20	6.8E18
N_{GA} (cm^{-3} eV^{-1})	8E13	1E16	1E12	1E12
E_{GA} (eV)	0.65	1.255	1.625	1.625
W_{TA} (eV)	0.01	0.01	0.01	0.01
W_{GA} (eV)	0.1	0.1	0.1	0.1
SIGTAE (cm^2)	5E-13	1E-10	5E-13	5E-13
SIGTAH (cm^2)	1E-15	1E-10	1E-15	1E-15
SIGGAE (cm^2)	5E-13	1E-10	5E-13	5E-13
SIGGAH (cm^2)	1E-15	1E-10	1E-15	1E-15

III. RESULTS AND DISCUSSIONS

A. Optimized simulations for CIGSe TFSC

Fig. 4 shows the schematic diagram of the JV curve for optimized simulation where solar cell parameters were inserted. The material parameters of each layer used in the CIGSe TFSC structure were optimized for obtaining high PCE. The optimized PCE for CIGSe TFSC from Silvaco Atlas was 21.92 %, which is slightly lower than the record PCE for CIGSe based TFSC (i.e., 23.35 %). The other solar cell parameters such as V_{oc}, J_{sc}, and FF for optimized conditions were 751.25 mV, 38.4 $mAcm^{-2}$, and 75.86 %, respectively. This result is in good agreement with other published results [4][11][15]. Fig. 4 displays the energy band diagram for CIGSe TFSC structure and recombination curve for optimized CIGSe TFSC. The recombination rate of TFSC depends on the quality of each layer used in the device. It is seen from Fig. 4b that the recombination rate was strongly enhanced when the CdS thickness increased. This growth of recombination rate at the high thickness of the CdS buffer layer is mainly due to the increase in the series resistance with the rising thickness of CdS [4]. The recombination rate in the CIGSe absorber layer remained almost constant and lowed up to 0.35 µm far from the junction. The recombination rate slightly starts to enhance when the charge carrier absorbs a distance more than 0.35 µm far from the junction. The rise in recombination far from the junction might be due to the back-surface recombination.

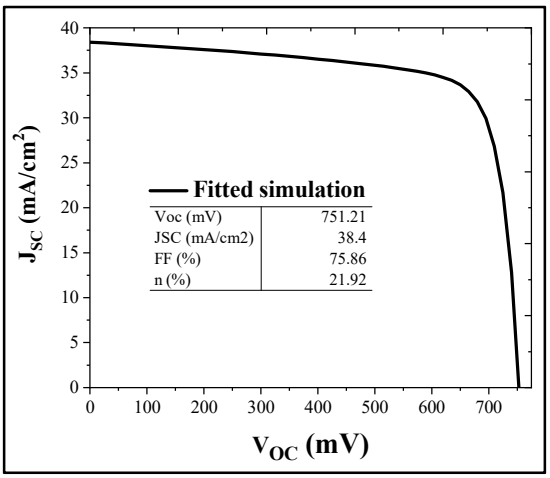

Fig. 3 Schematic of the JV curve for optimized simulation (Inserted a Table with solar cell parameters)

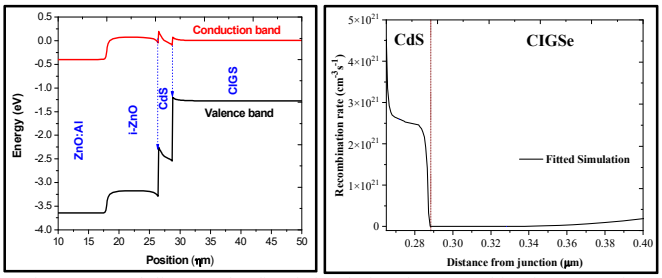

Fig. 4 a) Band diagram for fitted simulation. b) Recombination curve for optimized CIGSe TFSC measured at 500 mV

B. Experimental results for CIGSe thin films

Three different CIGSe thin films were deposited using the hybrid method at different first stage temperatures of 320, 330, and 340 ˚C. Various characterizations such as X-ray diffraction (XRD), Raman spectroscopy, scanning electron microscopy (SEM), atomic force microscope, and Hall Van der Pauw were performed to get the structural, morphological, and compositional information topographical, and electrical properties of CIGSe thin films, respectively. Fig. 5 shows the combined schematic diagram of XRD, Raman spectroscopy, SEM, AFM for CIGSe thin film

deposited by a hybrid deposition method. The experimentally obtained CIGSe thin films parameters were presented in Table III [12]. In XRD results, three strong peaks such as (112), (204/220), and (312)/(116) were seen [12]. These planes resemble the chalcopyrite crystal structure of CIGSe, which is verified by the international center for diffraction data (ICDD) number 083-3359 {with lattice constants, a = 5.6959 Å, and c = 11.3362 Å and c/a = 1.99}. The crystallite size of 25, 27.8, and 17.2 nm used the Debye-Scherrer equation for the samples CIGSe 320, CIGSe 330, and CIGSe 340, respectively. The intense A1 mode located at around 175 cm^{-1} from Raman spectroscopy is related to forming a stable and single CIGSe phase. The Raman spectroscopy verified the chalcopyrite crystal structure of CIGSe thin films because there are no other peaks present bear the A1 mode peak. The irregular size of grains with less than 1 µm was observed from the SEM images. From EDS results, the slightly copper poor composition of the films was found. The grain size for CIGSe thin film by AFM measurement was compatible with the grain size obtained from SEM. The average roughness of the CIGSe thin films deposited by the hybrid deposition method was less than 100 nm. The positive values of carrier concentration confirmed the formation of p-type semiconductors.

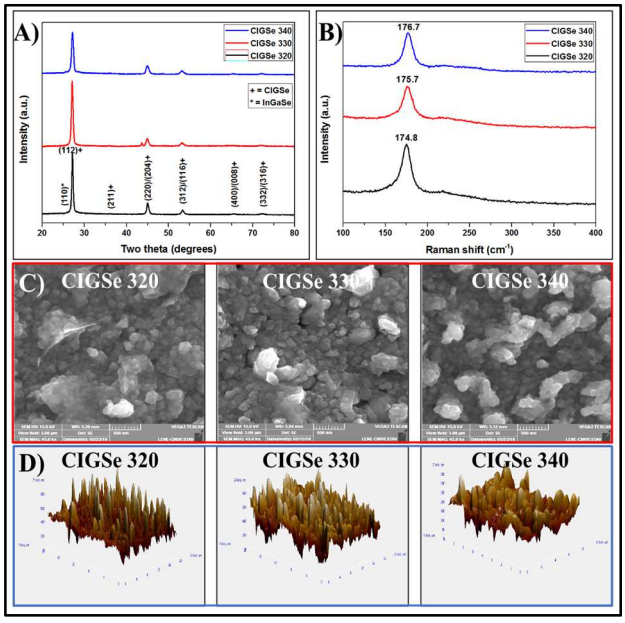

Fig. 5. Schematic of A) XRD, B) Raman spectroscopy, C) SEM, and D) AFM for CIGSe thin film deposited by hybrid deposition method

Table III. EXPERIMENTAL PARAMETERS OF CIGSe THIN FILMS DEPOSITED BY HYBRID DEPOSITION METHOD

Samples Parameters	CIGSe 320	CIGSe 330	CIGSe 340
Thickness (µm)	~1.3	~1.3	~1.3
(Ga/Ga+In)	0.37	0.44	0.36
Bandgap (eV)	1.24	1.28	1.23
Mobility (cm^2/V.s)	6.90	8.37	13.87
Concentration (cm^{-3})	4.2E16	8.3E16	2.5E16
Resistivity (Ω cm)	21.7	8.95	18

C. Simulating experimental results of CIGSe to the optimized simulation

In this case, the experimental parameters such as thickness, bandgap, mobility, concentration, and resistivity of CIGSe thin film deposited by the hybrid deposition method were replaced with the optimized condition. Fig. 6 showed the schematic of the JV curves for CIGSe thin films after replacing the experimental properties of CIGSe thin films. The device parameters of CIGSe TFSC for optimized condition and after replacing the experimental properties of CIGSe were presented in Table IV. This study was carried out to check how the device performance changes with experimental parameters than theoretical parameters. It can notice that the device performance has not altered after replacing the experimental parameters of CIGSe only. Therefore, the experimental parameters of the other layer must include getting a concise interpretation of the device performance. The recombination curves for CIGSe TFSC after replacing the experimental parameters of CIGSe thin films were depicted in Fig. 7. Similarly, the recombination rate was increased at a higher thickness of the CdS buffer layer [16]. The recombination rate was enhanced in the CIGSe absorber layer after a 0.34 µm distance from the junction. The recombination rate was very high for the sample CIGSe 330 ˚C showing that the samples having high gallium content contain a high recombination rate.

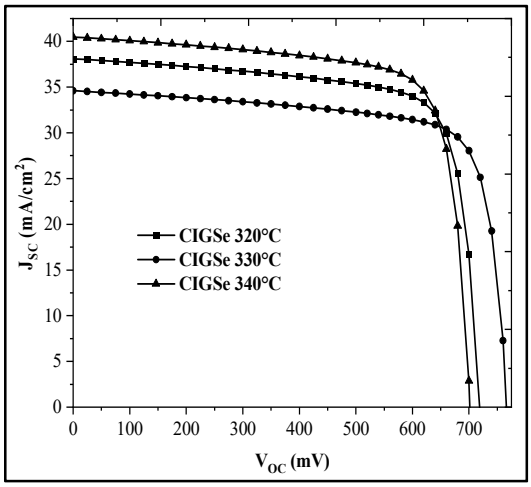

Fig. 6. Schematic of the J-V curves of CIGSe TFSC after replacing the experimental parameters of the CIGSe thin films

Table IV DEVICE PARAMETERS OF CIGSe TFSC FOR OPTIMIZED THICKNESS AND EXPERIMENTAL CIGSe THICKNESS

Device Parameters	CIGSe 320 °C (opt.)	CIGSe 320 °C (exp.)	CIGSe 330 °C (opt.)	CIGSe 330 °C (exp.)	CIGSe 340 °C (opt.)	CIGSe 340 °C (exp.)
V_{oc} (mV)	709.9	709.85	758.67	758.65	700.89	700.9
J_{sc} ($mAcm^{-2}$)	38.01	38.1	34.6	34.6	40.43	40.47
Fill factor (%)	75.48	75.49	75.89	75.89	75.68	75.68
Efficiency (%)	20.4	20.41	19.92	19.92	21.44	21.47

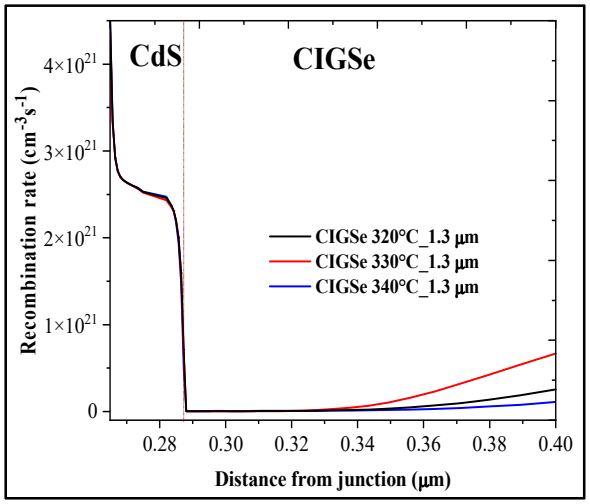

Fig. 7. Recombination curves for CIGSe TFSC after replacing the experimental parameters of the CIGSe thin films deposited at 320, 330, and 340°C

D. Simulating experimental results of CIGSe and CdS to the optimized simulation

Next, the simulation study focused on the CIGSe absorber and CdS buffer layers' experimental parameters. The practical details and obtained results for CdS thin films deposited by chemical bath deposition were taken from literature [17]. The CdS thin films were deposited at constant temperature of 80 ˚C and different times (i.e., from 20 to 60 minutes with the step of 10 ˚C). The solar cell parameters of the CIGSe TFSC after replacing the experimental parameters of CIGSe and CdS thin films. Table V showed the device parameters of CIGSe TFSC after replacing the experimental parameters of CIGSe and CdS thin films. Among various deposition condition of CdS thin films, the CdS thin films deposited at temperature of 80 ˚C for 20 minutes. This high performance is due to the very low thickness of CdS buffer layer. The J-V curves of CIGSe TFSC after replacing the experimental parameters of CIGSe and CdS (deposited at 80 ˚C for 20 minutes) thin films are shown in Fig. 8. The PCE of the three different CIGSe TFSC were 14.14, 14.79, and 13.77 % for CIGSe thin films deposited at 320, 330, and 340 ˚C, respectively [18]. The highest PCE for CIGSe 330 might be due to the high bandgap and high carrier concentration than other samples.

Fig. 9 depicts the recombination curves of the CIGSe TFSC after replacing the experimental parameters of CIGSe and CdS (deposited at 80 ˚C for 20 minutes) thin films. The very low recombination rate at CdS buffer layer was found showing thinner CdS buffer layer is needed for better performance. The recombination rate was enhanced with increase in the distance from the junction [16]. Although the recombination rate of CIGSe 330 was increased at a higher distance from the junction, the CIGSe 330 provides a better result because of the high quality of the material. By studying these properties in the simulation can guide to the experimental work.

Table V DEVICE PARAMETERS OF THE CIGSe TFSC AFTER REPLACING THE EXPERIMENTAL PARAMETERS OF CIGSe AND CdS THIN FILMS

Device Parameters	CdS CIGSe	CdS 80°C 20 min	CdS 80°C 30 min	CdS 80°C 40 min	CdS 80°C 50 min	CdS 80°C 60 min
Voc (mV)	CIGSe 320°C	722.63	722.15	528.78	726.78	737.31
Voc (mV)	CIGSe 330°C	771.23	776.63	779.17	778.09	586.6
Voc (mV)	CIGSe 340°C	706.00	511.28	714.64	713.97	723.76
Jsc (mAcm^{-2})	CIGSe 320°C	30.59	20.38	…	19.08	9.60
Jsc (mAcm^{-2})	CIGSe 330°C	27.97	19.46	17.08	19.37	…
Jsc (mAcm^{-2})	CIGSe 340°C	32.50	…	16.11	18.53	9.30
FF (%)	CIGSe 320°C	63.97	48.40	…	57.31	53.83
FF (%)	CIGSe 330°C	68.57	47.86	53.14	58.12	…
FF (%)	CIGSe 340°C	60.03	…	52.87	56.63	53.93
η (%)	CIGSe 320°C	14.14	7.12	…	7.95	3.81
η (%)	CIGSe 330°C	14.79	7.23	7.07	8.76	…
η (%)	CIGSe 340°C	13.77	…	6.09	7.49	3.69

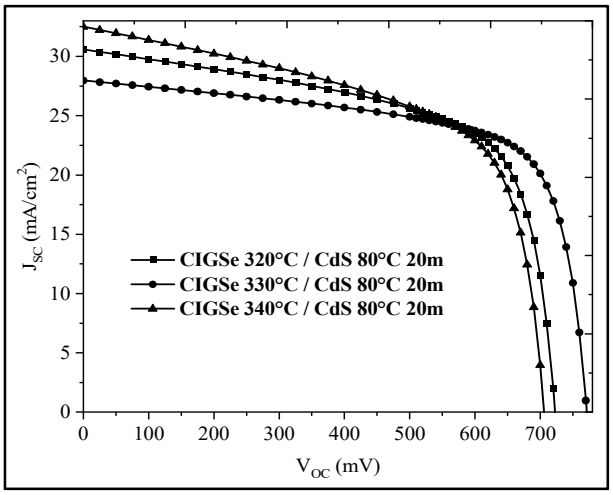

Fig. 8 schematic of the J-V curves of CIGSe TFSC after replacing the experimental parameters of CIGSe and CdS (deposited at 80 ˚C for 20 minutes) thin films

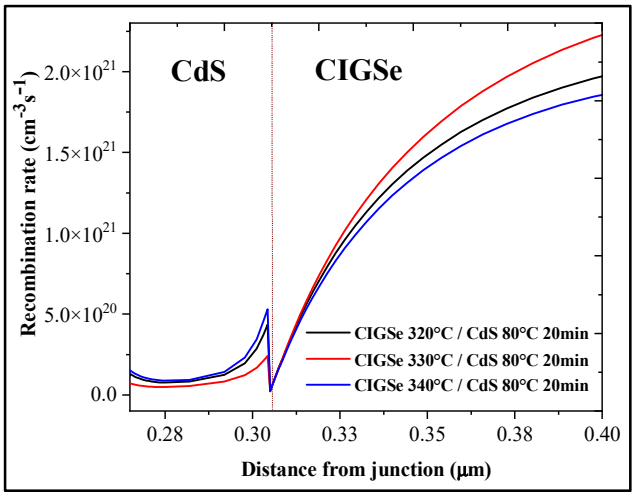

Fig. 9 Recombination curves of the CIGSe TFSC after replacing the experimental parameters of CIGSe and CdS (deposited at 80 ˚C for 20 minutes) thin films

IV. CONCLUSION

In summary, the Silvaco ATLAS simulation was carried out for optimizing the CIGSe TFSC structure. The influence of various parameters such as thickness, bandgap, carrier concentration, and electron affinity of each layer used in CIGSe TFSC was studied and optimized for high performance. The optimized PCE for CIGSe TFSC was 21.92 %. The experimental results of CIGSe and CdS thin films were replaced to the optimized conditions. The device performance and recombination rate were thoroughly investigated. There was no variation in the device performance after replacing the experimental parameters of CIGSe only. The PCE of CIGSe TFSC drastically degraded to around 14 %, indicating that material parameters control the device performance. The recombination rate is enormously increased if the CdS thickness enhances. And recombination rate is high at the CIGSe absorber layer higher distance from the junction. By analyzing the device performance and the recombination rate, the simulation can optimize the materials parameters for high performance. This study can provide information for doing practical work.

ACKNOWLEDGEMENT

The authors would like to thank the Consejo Nacional de Ciencia y Technlogıá-Secretarıá de Energıá (CONACYT) for financial support. The authors are also grateful to the CINVESTAV-IPN and Universidad de Ciencias y Artes de Chiapas for providing a place to investigate and finish the project. We would like to acknowledge the people from the section of solid-state electronics of CINVESTAV-IPN, namely Jaime Vega Perez, Miguel A. Avendaño Ibarra, Norma Iris Gonzalez Garcia, Miguel Galvan Arellano, Eduardo Pérez Garduño, Adolfo Tavira, Yesenia Cervantes Aguirre, Jose Martin Jimenez Sarmiento, etc. for their valuable support.

REFERENCES

[1] S. Mughal, Y. R. Sood, and R. K. Jarial, “A Review on Solar Photovoltaic Technology and Future Trends,” NCRACIT) Int. J. Sci. Res. Comput. Sci. Eng. Inf. Technol. © 2018 IJSRCSEIT, vol. 1, no. 4, pp. 227–235, 2018.

[2] G. Regmi, A. Ashok, and S. Velumani, “Perspectives of chalcopyrite-based CIGSe thin-film solar cell: a review,” J. Mater. Sci. Mater. Electron., 2020.

[3] M. Green, E. Dunlop, J. Hohl-Ebinger, M. Yoshita, N. Kopidakis, and X. Hao, “Solar cell efficiency tables (version 57),” Prog. Photovoltaics Res. Appl., vol. 29, no. 1, pp. 3–15, 2021.

[4] S. Dabbabi, T. Ben Nasr, and N. Kamoun-Turki, “Parameters optimization of CIGS solar cell using 2D physical modeling,” Results Phys., vol. 7, pp. 4020–4024, 2017.

[5] A. Kowsar, M. Billah, S. Dey, S. C. Debnath, S. Yeakin, and S. F. Uddin Farhad, “Comparative Study on Solar Cell Simulators,” ICIET 2019 - 2nd Int. Conf. Innov. Eng. Technol., pp. 23–24, 2019.

[6] S. Michael and A. Bates, “The design and optimization of advanced multijunction solar cells using the Silvaco ATLAS software package,” Sol. Energy Mater. Sol. Cells, vol. 87, no. 1–4, pp. 785–794, 2005.

[7] A. Ashok, G. Regmi, and S. Velumani, “Characterizations of a Selenized Cu(In1-xGax)Se2 Thin Film Absorber Layer Fabricated By a Three-Stage Hybrid Method,” in 15th International Conference on Electrical Engineering, Computing Science and Automatic Control (CCE), 2018.

[8] A. Ashok, G. Regmi, and S. Velumani, “Growth of In2Se3Thin Films Prepared by the Pneumatic Spray Pyrolysis Method for Thin Film Solar Cells Applications,” 17th Int. Conf. Electr. Eng. Comput. Sci. Autom. Control. CCE 2020.

[9] J. M. Delgado-Sanchez et al., “Front contact optimization of industrial scale CIGS solar cells for low solar concentration using 2D physical modeling,” Renew. Energy, vol. 101, pp. 90–95, 2017.

[10] A. Saharia, R. K. Maddila, J. Ali, P. Yupapin, and G. Singh, “An elementary optical logic circuit for quantum computing: a review,” Opt. Quantum Electron., vol. 51, no. 7, pp. 1–13, 2019.

[11] N. E. I. Boukortt, S. Patanè, and Y. M. Abdulraheem, “Numerical investigation of CIGS thin-film solar cells,” Sol. Energy, vol. 204, no. May, pp. 440–447, 2020.

[12] D. Valencia, J. Conde, A. Ashok, and S. Velumani, “Optimization of Cu(In, Ga)Se2 (CIGSe) thin film solar cells parameters through numerical simulation and experimental study,” Sol. Energy, 2021.

[13] S. K. Pandey, “Enhanced performance and defect analysis of mgzno based CIGS solar cell,” J. Nanoelectron. Optoelectron., vol. 11, no. 5, pp. 649–655, 2016.

[14] I. E. Tinedert, F. Pezzimenti, M. L. Megherbi, and A. Saadoune, “Design and simulation of a high efficiency CdS/CdTe solar cell,” Optik (Stuttg)., vol. 208, no. December 2019, p. 164112, 2020.

[15] A. Khadir, “Simulation of Effects of Defects and Layers Thickness on the Performance of CIGS Solar Cells,” vol. 137, no. 6, pp. 1128–1134, 2020.

[16] N. Amin, P. Chelvanathan, M. I. Hossain, and K. Sopian, “Numerical modelling of ultra thin Cu(In,Ga)Se 2 solar cells,” Energy Procedia, vol. 15, no. 2011, pp. 291–298, 2012.

[17] A. Ashok, G. Regmi, and S. Velumani, “Comparative studies of CdS thin films by chemical bath deposition techniques as a buffer layer for solar cell applications,” J. Mater. Sci. Mater. Electron., 2020.

[18] Valencia, D., Conde, J., Ashok, A., Meza-Avendaño, C. A., Vilchis, H., & Velumani, S. “Optimization of Cu (In, Ga) Se2 (CIGSe) thin film solar cells parameters through numerical simulation and experimental study”. *Solar Energy*, *224*, 298-308. 2021.